An optimized dissolved oxygen concentration control in SBR with the use of adaptive and predictive control schemes

Tomasz Zubowicz[1], Tomasz Ujazdowski[1], Zuzanna Klawikowska[1], and Robert Piotrowski[1]

***Abstract*— This paper addresses the problem of optimizing control of the aeration process in a water resource recovery facility (WRRF) using sequencing batch reactor (SBR), one that affects the efficiency of wastewater treatment by stimulating metabolic reactions of microorganisms through dissolved oxygen (DO) level control, and accounts for the predominant part of operating costs. Two independent approaches to DO control algorithm design based on nonlinear model-based predictive control (NMPC) with constraints and direct model reference adaptive control (DMRAC) are proposed and compared. Both algorithms were developed on the basis of utility models obtained by cognitive model simplification, however, both algorithms are characterized by a distinct mechanism to achieve control optimality and incorporate uncertainty. The NMPC-based algorithm solves an online optimization task by reducing the impact of uncertainty through feedback and estimating its influence by evaluating the differences between the internal model and measurements on a sliding prediction window. In contrast, DMRAC reduces the impact of uncertainty through the adaptation of control law parameters. Meanwhile, optimality is encoded in the reference model parameters reflecting the operation of the closed-loop system and in the independent parameters of the adaptation mechanism. Illustrations of the algorithms' operation were provided by simulation experiments using a three-layer SBR model of the Swarzewo wastewater treatment plant with ASM3e-based reactions.**

I. INTRODUCTION

Emerging state-of-the-art technologies used in water resource recovery facilities (WRRFs) are associated not only with continuous flow reactors, but rather with sequencing batch reactors (SBRs) [1]. The latter are considered to provide a flexible approach to plant design and high operational performance for both municipal and industrial wastewater treatment [2]. Contributing to this fact is, among others, the recent development of measurement equipment and automation solutions resulting in increased efficiencies achieved and operational cost reduction of more than 60% compared to traditional activated sludge processes [3].

A SBR treatment duty cycle, typically, employs five operating phases [4]. These include filling, reaction, settling, decantation, and, in some cases omitted, idle phases. Scheduling of phases is aimed at achieving operational goals related to contaminant removal. It is associated individually with the plant and very often optimized. The observed variations depend on the characteristics of the treatment plant and the influent wastewater [5].

The control of the processes involved in the distinct phases of SBR treatment is usually divided according to quantitative and qualitative aspects, with interaction from the former to the latter [6]. One of the key factors affecting performance and running costs is that related to the reaction phase and control of the aeration process maintaining the desired dissolved oxygen (DO) concentration level. The scope of the paper is focused on a group of algorithms capable of achieving an optimizing DO control in SBR. For this purpose, a predictive and an adaptive control algorithms with an internal model are considered. These include model-based predictive control (MPC) and direct model reference adaptive control (DMRAC) families. The former one is characterized by recursive optimization of control signal values, thus influencing the control quality index. The algorithm responds to changes in the environment, reducing uncertainty through information from feedback. The advantage of this approach is that there is no need to develop a control law structure, while the disadvantage is the need to guarantee the admissibility of the solution on a receding horizon. The DMRAC, on the other hand, modifies the parameters of the control system through the use of feedback thus reducing the influence of uncertainty. The algorithm attempts to maintain the desired — optimal — behavior of the closed-loop system encoded in the form of a reference model. The advantage of DMRAC is that the optimization task is reduced to solving differential equations, namely adaptation laws, whereas the disadvantage is the need to develop the structure of the control law. Also, even in case of the linear systems, the DMRAC nature is non-linear and may manifest through additional oscillations in the system. However, with a suitable configuration of the two algorithms, both can solve a analogous optimization task guaranteeing comparable performance, as will be shown in this article..

The MPC approach to DO in WRRF control finds its origins and majority of works concerning the continuous-flow facilities. An MPC based DO control taking under consideration internal recycle flow was presented in [7]. An approach incorporating the aeration (actuator) system model was proposed in [8]. A multivariate MPC approach incorporating effluent ammonia concentration measurement was proposed in [9]. An adaptive MPC scheme with targeting only aerobic reactors has been investigated in [10]. In [11], a nonlinear model-based predictive control (NMPC) approach was proposed and tested on a benchmark model [12]. An adaptive fuzzy neural network-based MPC was used for DO

*Financial support from Gdańsk University of Technology by the DEC-43/2021/IDUB/I.3.3 grant under the Argentum Triggering Research Grants - 'Excellence Initiative - Research University' program is gratefully acknowledged.

[1]Tomasz Zubowicz, Tomasz Ujazdowski, Zuzanna Klawikowska and Robert Piotrowski are with Dept. of Intelligent Control Systems and Decision Support, Gdańsk University of Technology, 80-233 Gdańsk, Poland

[1] tomasz.zubowicz@pg.edu.pl

control and tested using BMS2 in [13]. In turn, a MPC approach focused on minimizing global warming potential or the amount of pollution was proposed and tested using activated sludge model no. 1 (ASM1) based SBR in [14].

Application of the DMRAC type algorithms to DO control has been investigated with respect to both continuous-flow and batch type facilities. A performance comparison of DMRAC and NMPC in terms of DO trajectory tracking in continuous-flow reactors was proposed in [15]. An extension of the approach with the use of adjusted on-line parameter estimation mechanism was proposed in [16]. An application of DMRAC with anti-windup to DO control in SBR was presented in [17]. A step-wise adaptation of DMRAC parameters was investigated in [18]. A hierarchical DMRAC structures for DO control in SBR were studied in [19].

The contribution of this research work is as follows. Two algorithms, namely NMPC with constraints and DMRAC were presented together with a method for their configuration. Both allow to achieve optimized control of DO concentration in the SBR aimed at the trajectory tracking performance of the set trajectory. This provides a novel perspective on DMRAC as a tool delivering an optimizing control algorithm, which distinguishes the proposed approach from those known in the literature. In addition, simulation experiments were carried out comparing the performance of both algorithms on a calibrated model of a SBR plant in Swarzewo under uncertainty arising from the realization of input disturbances.

The remainder of the paper is constructed as follows. In Section II a problem formulation is presented. In Section III cognitive and utility models for simulation and control design are provided. Subsequently, the control algorithm derivation is described in Section IV. Results of the numerical studies are presented in Section V. Section VI concludes the paper.

II. PROBLEM FORMULATION

Suppose $\mathbb{R}^n$ is to represent a vector space over a field of real numbers $\mathbb{R}$ with usual addition $(+)$, scalar multiplication $(\cdot)$, Cartesian product $(\times)$, and $\mathbb{T} \subset \mathbb{R}$ denotes an open set. Taking a set of elements from a positive part of an integer field, $\{n_{\mathrm{x}}, n_{\mathrm{u}}, n_{\mathrm{d}}, n_{\mathrm{y}}, n_{\mathrm{c}}\} \subset \mathbb{Z}_+$, enables one to construct an n-tuple of vector valued functions $\mathbb{T} \to \mathbb{R}^n$ such that $\forall t \in \mathbb{T}$ it follows that $(\boldsymbol{x}(t), \overline{\boldsymbol{u}}(t), \boldsymbol{d}(t), \boldsymbol{y}(t), \boldsymbol{c}(t)) \in (\mathbb{X}_{\mathrm{x}}, \mathbb{X}_{\overline{\mathrm{u}}}, \mathbb{X}_{\mathrm{d}}, \mathbb{X}_{\mathrm{y}}, \mathbb{X}_{\mathrm{c}}) \subset (\mathbb{R}^{n_{\mathrm{x}}}, \mathbb{R}^{n_{\mathrm{u}}}, \mathbb{R}^{n_{\mathrm{d}}}, \mathbb{R}^{n_{\mathrm{y}}}, \mathbb{R}^{n_{\mathrm{c}}})$. In particular t is to denote time. In consequence, a mathematical model (Σ_{SBR}) of a physical plant is defined as:

$$\Sigma_{\mathrm{SBR}} : \begin{cases} \mathbb{X}_{\mathrm{x}} \times \mathbb{X}_{\overline{\mathrm{u}}} \times \mathbb{X}_{\mathrm{d}} \to \mathbb{R}^{n_{\mathrm{x}}} \\ \mathbb{X}_{\mathrm{x}} \times \mathbb{X}_{\overline{\mathrm{u}}} \times \mathbb{X}_{\mathrm{d}} \to \mathbb{X}_{\mathrm{y}} \\ \mathbb{X}_{\mathrm{x}} \times \mathbb{X}_{\overline{\mathrm{u}}} \times \mathbb{X}_{\mathrm{d}} \to \mathbb{X}_{\mathrm{c}} \end{cases}, \tag{1}$$

where $\mathbb{X}_{\mathrm{x}}$, $\mathbb{X}_{\overline{\mathrm{u}}}$, $\mathbb{X}_{\mathrm{d}}$, $\mathbb{X}_{\mathrm{y}}$, $\mathbb{X}_{\mathrm{c}}$ are used to denote operating regions in the state, control and disturbance input, measured and controlled output spaces, respectively.

The measurement system providing soft-sensor measurements is given by:

$$\Sigma_{\mathrm{M}} : \mathbb{X}_{\mathrm{y}} \times \mathbb{X}_{\mathrm{d}} \to \mathbb{X}_{\mathrm{y_m}}. \tag{2}$$

The control signals affect the plant through an actuators system as:

$$\Sigma_{\mathrm{A}} : \mathbb{X}_{\mathrm{u}} \to \mathbb{X}_{\overline{\mathrm{u}}}, \tag{3}$$

where $\mathbb{X}_{\overline{\mathrm{u}}} \subseteq \mathbb{X}_{\mathrm{u}} \ni \boldsymbol{u}(t)$, $\forall t$.

The objective is to design a control system for the aeration process Σ_{DO}, a component of the plant-wide control system Σ_{C}, which, $\forall t$, maps measurements ($\boldsymbol{y}_{\mathrm{m}}(t) \in \mathbb{X}_{\mathrm{y_m}} \subset \mathbb{X}_{\mathrm{y}}$) and reference trajectories ($\boldsymbol{r}(t) \in \mathbb{X}_{\mathrm{r}} \subset \mathbb{X}_{\mathrm{c}}$) into control signals:

$$\mathbb{X}_{\mathrm{u}} \leftarrow \Sigma_{\mathrm{A}} \circ \Sigma_{\mathrm{C}} \circ \Sigma_{\mathrm{M}} \left[\mathbb{X}_{\mathrm{y_m}} \times \mathbb{X}_{\mathrm{r}}\right], \tag{4}$$

where $\circ$ denotes a composition operator.

Closing the loop over (1) by (4) yields the control scheme as illustrated in Fig. 1.

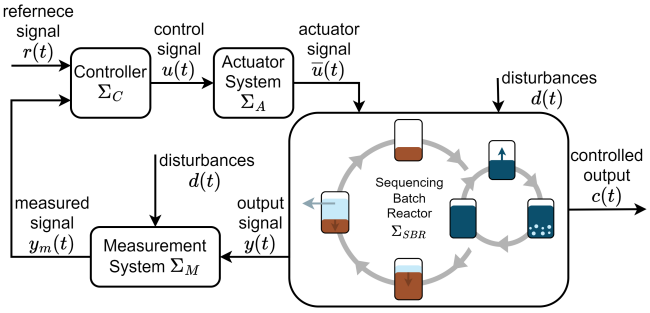

Fig. 1. Scheme of control system.

To this end two methods for designing an optimizing Σ_{DO} are considered, namely NMPC as DMRAC.

The scope of the approach is set by adopting the following assumptions.

Assumption 1: The plant is considered to operate under normal operating state and conditions.

Under Assumption 1 only a daily basis plant operation is considered. Also, this is to account for the disturbance inputs profiles. Any fault or process anomaly is considered to be handled by separate operational control mode.

Assumption 2: Bioreactor inflow is characterized by cubic flow (Q) and aggregated quality measures: chemical oxygen demand (COD), total nitrogen (TN), and total phosphorus (TP).

Assumptions 1 – 2 enable one to define an experiment scenario configuration using data collected on-site, during typical measurement campaign.

Assumption 3: The utility model uncertainties can be represented using a constant or slowly time-varying additive term.

The Assumption 3 remains valid for DO concentration control as demonstrated in [20].

Assumption 4: The influence of biological species on DO dynamics is represented by respiration rate which can be estimated with sufficiently high accuracy.

Assumption 4 is met by implementing results provided in [21] or using more sophisticated solution [22].

III. MODELING

In Section III-A a cognitive model of SBR is described. Sections III-B details the sensor and actuator models. Process utility models for MPC and DMRAC algorithm purposes are given in Section III-C. A DMRAC reference model is provided in Section III-D.

A. Plant model for simulation purposes

The fundamental model for predicting phenomena occurring in the SBR, namely first component of (1), is given by the continuity equation as:

$$\partial_t \rho(\boldsymbol{a}, t) + \nabla \cdot (\rho(\boldsymbol{a}, t)\boldsymbol{u}_{\mathrm{CS}}) - q(\boldsymbol{a}, t) = 0, \tag{5}$$

where the time variation (∂_t) of medium quality component being considered $\rho(\boldsymbol{a}, t)$ at a given point in space $\boldsymbol{a}$ depends on the transportation $\nabla \cdot (\rho(\boldsymbol{a}, t)\boldsymbol{u}_{\mathrm{CS}})$ and reaction term $q(\boldsymbol{a}, t)$ in Petersen–Gujer form that implements the extended activated sludge model no. 3 (ASM3e) [23]. The spatial component is typically restricted to z-axis oriented along the acting gravity force, hence, it follows that $\nabla \stackrel{\text{def}}{=} \partial_z$ and $\boldsymbol{u}_{\mathrm{CS}} \stackrel{\text{def}}{=} v_z$ [23].

Given the above provisions, Assumption 1, and adopting the spatial discretization method through variable volumes, the (5) is simplified and unraveled numerically to predict the evolution of ρ. Combining the mass balance equation to account for the medium volume with the evolution of ρ for all considered bio-chemical species in each discrete volume is to represent $\boldsymbol{x}$. Including the SBR inflow under Assumption 2 yields $\boldsymbol{d}$. Combining air inflow, mixer, wastewater feed and outflow pumps operation accounts for $\boldsymbol{u}$. Thus Σ_{SBR} defined in (1) is obtained, according to [23].

B. Sensor and actuator models

The measurement system Σ_{M} comprises two parts. First, a classical current output loop (4–20 mA) sensor model incorporating the impact of the quantization processes, measurement noise or the conversion of the analogue signal to digital was used to assess the impact of the DO measurement quality [22]. Second, by the virtue of Assumption 4, a respiration rate estimator was assumed available as part of the measurement system.

The actuator system model Σ_{A} implementing a simplified representation of air blowers and connected piping of the aeration system in the form of a saturation non-linearity was used. The maximum flow rate from the blower ($u_{\max}$) was set for the nominal pressure at the operating point. In addition, warnings in the event of blower overheating or surge have also been implemented.

C. Plant model for control design

Let the dynamics of DO in a discrete variable volume of Σ_{SBR} containing an immersed probe be of the form:

$$\begin{aligned} \mathrm{d}_t\, C_{\mathrm{O}_2} = {} & f_T(T(t))\, \alpha\, k_l a_{20}\ (Q_{\mathrm{air}}(t), h(t)) \\ & (C_{\mathrm{O}_2\,\mathrm{sat}}(T(t)) - C_{\mathrm{O}_2}(t)) - \overline{R}(t) + \overline{\Phi}_{\mathrm{m}}(t), \end{aligned} \tag{6}$$

where $T(t)$ signifies temperature at t; $f(T(t)) \stackrel{\text{def}}{=} 1.024^{(T(t)-20)}$ accounts for Arrhenius equation; α is the oxygen transfer coefficient; $k_l a_{20}$ denotes the aeration rate dependent on the airflow ($Q_{\mathrm{air}}(t)$) and height of medium level ($h(t)$) in the SBR, $C_{\mathrm{O}_2\,\mathrm{sat}}(T(t))$ signifies cubic approximation of temperature-dependent DO saturation level, $\overline{R}(t) \stackrel{\text{def}}{=} \frac{DO(t)}{K+DO(t)} R(t)$ is the rate of respiration ($R(t)$) to account for the impact of biological species on the DO balance in ASM3e, $\overline{\Phi}_{\mathrm{m}}(t)$ represents the impact of internal mixing flows from neighboring SBR layers [23], and:

$$k_l a_{20}(Q_{air}(t), h(t)) \stackrel{\text{def}}{=} R_{20}\, \frac{h(t) - h_{\mathrm{diff}}}{C_{\mathrm{O}_2\,\mathrm{sat}}(20)\, V_{\max}}\, Q_{\mathrm{air}}(t), \tag{7}$$

with: R_{20} representing the oxygen flow at nominal temperature, h_{diff} the immersion depth of diffusors, and $V_{\max}$ as the maximum tank volume.

Following the justification of Assumption 4, the respiration rate estimator provides information on $\hat{R}(t) = \overline{R}(t) + \overline{\Phi}_{\mathrm{m}}(t)$, thus (6) is rewritten as $\Sigma_{\mathrm{SBR-DMRAC}}$:

$$\begin{aligned} \mathrm{d}_t\, C_{\mathrm{O}_2} = {} & f_T(T(t))\, \alpha\, k_l a_{20}\ (Q_{air}(t), h(t)) \\ & (C_{\mathrm{O}_2\,\mathrm{sat}}(T(t)) - C_{\mathrm{O}_2}(t)) - \hat{R}(t), \end{aligned} \tag{8}$$

which provides basis for the derivation of DMRAC.

Given the nominal parameter values are available through Σ_{SBR} calibration and the Assumption 3 holds true, then, by applying forward Euler discretization method to (6) the $\Sigma_{\mathrm{SBR-MPC}}$ yields:

$$\begin{cases} x_0 & = x_{\mathrm{I}} \\ y_k & = x_k \\ x_{k+1} & = x_k + T_{\mathrm{s}}\, f_T(d_{1\,k})\, \alpha\, k_l a_{20}(u_k,\, d_{2\,k}) \\ & \qquad (C_{\mathrm{O}_2\,\mathrm{sat}}(d_{1\,k}) - x_k) - T_{\mathrm{s}}\, d_{3\,k} + d_{4\,k} \end{cases}, \tag{9}$$

where x_{I} is the initial state, $(x_k,\, u_k) \equiv (C_{\mathrm{O}_2}(t),\, Q_{\mathrm{air}}(t))|_{t=kT_{\mathrm{s}}}$ denote the internal model state and control input, $(d_{1\,k}, d_{2\,k}, d_{3\,k}) \equiv (T_k, h_k,\, \hat{R}_k)$ are disturbance inputs, namely measured temperature, medium level, and respiration rate estimate, with respect to Assumption 4, and $d_{4\,k}$ is to account for modeling uncertainties arising due to structure and parameter errors, y_k denotes the output.

Remark 1: The $d_{4\,k}$ term aggregates the impact of transforming (6) into (9) as well as the Σ_{SBR} parameter identification error.

D. Closed-loop reference model for adaptive control

Closed-loop reference trajectory $y_r(t)$ is arbitrarily expressed by the model reference dynamics:

$$\mathrm{d}_t\, y_{\mathrm{r}}(t) = -a_{\mathrm{m}} y_r(t) + b_{\mathrm{m}} r(t) \tag{10}$$

where $y_{\mathrm{r}}(t)$,$r(t)$ represent the reference model output and input (reference signal), respectively, a_{m}, b_{m} denote the model parameters that encode desired close-loop system behavior.

IV. CONTROL SYSTEM DESIGN

Two optimizing control strategies are considered. First, an NMPC approach to algorithm design is presented in Section IV-A. Second, a DMRAC scheme is configured as described in Section IV-B.

A. Nonlinear model-based predictive control

A scheme of the NMPC controller with reference to Fig. 1 is presented in Fig. 2.

Let the control, disturbance, and output sequences over a prediction horizon N be given by:

$$\mathcal{U}_k = [u(k|k)\ u(k+1|k)\ \dots\ u(k+N-1|k)]^T, \quad (11a)$$

$$\mathcal{D}_k = [\boldsymbol{d}(k|k)^T\ \boldsymbol{d}(k+1|k)^T\ \dots\ \boldsymbol{d}(k+N-1|k)^T]^T, \quad (11b)$$

$$\mathcal{Y}_k^T = [y(k|k)\ y(k+1|k)\ \dots\ y(k+N-1|k)]^T. \quad (11c)$$

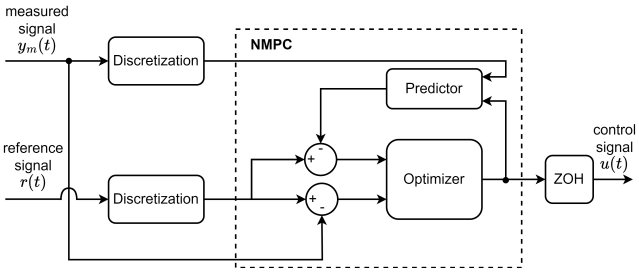

Fig. 2. NMPC scheme.

At each k over the experiment horizon (T_E) the NMPC, based on the soft-measurement feedback and disturbance predictions $\mathcal{D}_k$, solves a non-linear model based optimization task with constraints to produce $\mathcal{U}_k$. Only the first element of $\mathcal{U}_k$ is applied to plant as a control input using Σ_A, as:

$$u(t) = \mathcal{L}_\mathrm{ZOH}\left\{u^*(k|k)\right\}, \quad (12)$$

where $(\cdot)^*$ is optimal realization of $(\cdot)$, $\mathcal{L}_\mathrm{ZOH}$ denotes a signal reconstruction using zero-order-hold digital to analog converter.

Elements in $\mathcal{U}_k \in \mathbb{X}_\mathrm{u}$ due to Σ_A. Also, the $\mathcal{Y}_k \in \mathbb{X}_\mathrm{y}$, where the lower ($y_\mathrm{min}$) and upper ($y_\mathrm{max}$) bound on DO concentration is zero and $C_{\mathrm{O_2\,sat\,20}}$, respectively. For practical reasons, the NMPC implementation includes variables normalization (s) and (non-negative) slack variable ε, through which the input (Ω_u) and output (Ω_y) constraints, $\forall k, p$ over the experiment and prediction horizons, yield:

$$\frac{y_\mathrm{min}}{s^y} - \varepsilon_k V^y_\mathrm{min}(p) \le \frac{y(k+p \mid k)}{s^y} \le \frac{y_\mathrm{max}}{s^y} + \varepsilon_k V^y_\mathrm{max}(p), \quad (13a)$$

$$\frac{u_\mathrm{min}}{s^u} - \varepsilon_k V^u_\mathrm{min}(p) \le \frac{u(k+p-1 \mid k)}{s^u} \le \frac{u_\mathrm{max}}{s^u} + \varepsilon_k V^u_\mathrm{max}(p). \quad (13b)$$

where V denotes a dimensionless sequences used to soften the constraints. The inclusion of variable normalization and slack variables in NMPC implementations addresses practical concerns about scaling issues and constraint violations. Normalization helps to deal with scaling differences in variables, improves the numerical conditioning of the whole algorithm, and reduces the problem of task sensitivity. In addition, since each search direction is equal, it allows for better exploration of solutions. Slack variables provide a relaxation of hard constraints, increasing feasibility and robustness in real-world applications, and provide a non-empty set of admissible solutions, especially when initializing the algorithm. The disadvantage of using such a solution is that these constraints may be exceeded when a boundary solution is obtained.

Due to technological SBR setup, namely a vast impact of uncertainty related to processes which influences the time realization of disturbances in relation to the slow dynamics of the process [24], the disturbance prediction $\mathcal{D}_k$ is produced as a constant value extrapolation over N using soft-measurements at k and previous step model output y_{k-1}.

Taking $\boldsymbol{z}_k \stackrel{\mathrm{def}}{=} [\mathcal{U}_k^T,\ \epsilon_k]^T$ as a vector of decision variables, a cost function J is defined by considering the output tracking performance and impact of ε as:

$$J(z_k) = \sum_{p=1}^{N}\{[r(k+p|k) - y(k+p|k)]^2\} + \rho_\varepsilon \varepsilon_k^2, \quad (14)$$

where ρ_ε is a weighting factor.

Then the optimization problem takes the form of:

$$\begin{aligned} J^* = \min_{\boldsymbol{z}_k} & J(\boldsymbol{z}_k) \\ \text{s.t.}\quad & \mathcal{D}_k \leftarrow \Sigma_\mathrm{D}[y_{0\,k-1}, y_{\mathrm{m}\,0\,k}], \\ & \mathcal{Y}_k \leftarrow \Sigma_{\mathrm{SBR-MPC}}[\mathcal{U}_k, \mathcal{D}_k, x_{0\,k}], \\ & x(k+N|k) = x_\mathrm{N}, \\ & \mathcal{U}_k \in \Omega_\mathrm{u}, \mathcal{Y}_k \in \Omega_\mathrm{y}, \varepsilon_k \ge 0, \end{aligned} \quad (15)$$

where $x_{0\,k}$ is acquired from measurements at k.

Remark 2: Given h in $\Sigma_{\mathrm{SBR-MPC}}$ such that $h(x,u) \ge 0$ and $h(x,u) = 0$ if and only if $x = 0$ and $u = 0$, the algorithm stability holds true due to terminal constraint [25].

Combining the above derivations yields the $\Sigma_{\mathrm{DO-MPC}}$.

B. Adaptive scheme for optimizing control

A scheme of the DMRAC controller with reference to Fig. 1 is presented in Fig. 3.

The inherent property of the DMRAC algorithm is to enable tracking control in the presence of uncertain or time-varying plant parameters. Two 'degrees' of freedom are available to a designer's choice. These include, reference model parameters and controller parameter adaptation rate gains. In the following sections both are used to adopt optimizing control behavior.

Given (8), the proposed control law yields:

$$u(t) = \theta_\mathrm{y}(t)\, y(t) + \theta_\mathrm{R}(t)\hat{R}(t) + \theta_\mathrm{r}(t) r(t), \quad (16)$$

where $y(t)$, $r(t)$ are the continuous-time counterparts of signals defined in (9) and $\theta_{(\cdot)}(t)$ denote the time-varying controller gains related to $(\cdot)$ controller input.

The (16) is verified as well-parameterized due to existence of the ideal parameters given by:

$$\underline{\theta}_\mathrm{y}(t) = \frac{-a_\mathrm{m}}{b_\mathrm{p}(t)},\ \underline{\theta}_\mathrm{R}(t) = \frac{1}{b_\mathrm{p}(t)},\ \underline{\theta}_\mathrm{r}(t) = \frac{b_\mathrm{m}}{b_\mathrm{p}(t)}. \quad (17)$$

where $b_p(t) \stackrel{\mathrm{def}}{=} \overline{\alpha}\,(C_{\mathrm{O_2\,sat}}(T(t)) - C_{\mathrm{O_2}}(t))$ and $\overline{\alpha}$ is the combined term of α and (7).

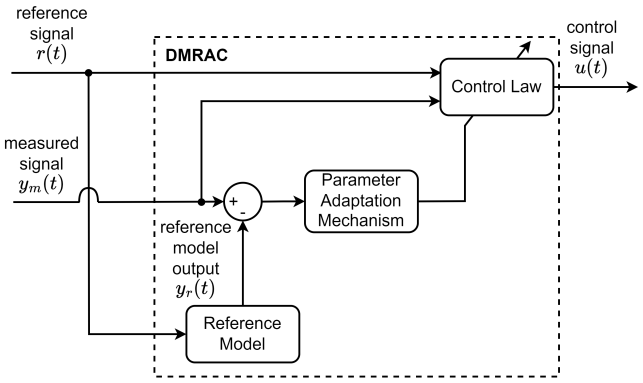

Fig. 3. DMRAC scheme.

Let $e(t) \stackrel{\text{def}}{=} y(t) - r(t)$ denote a tracking error. Then the system obtained by closing the loop over (8) using (16) remains stable with a Lyapunov function given by:

$$V(e(t), \boldsymbol{\theta}(t)) = (e(t))^2 + (\boldsymbol{\theta}(t))^T \boldsymbol{P}_\gamma \boldsymbol{\theta}(t), \tag{18}$$

where $\boldsymbol{\theta} \stackrel{\text{def}}{=} [\theta_\text{y}, \theta_\text{R}, \theta_\text{r}]^T$ and $\boldsymbol{P}_\gamma \stackrel{\text{def}}{=} \text{diag}\,(\gamma_1, \gamma_2, \gamma_3)$ is a positive definite matrix, if the adaptation mechanism is selected as:

$$\text{d}_t\, \boldsymbol{\theta}(t) = -e(t)\boldsymbol{\gamma}^T \boldsymbol{\phi}(t) \tag{19}$$

where $\boldsymbol{\phi} \stackrel{\text{def}}{=} \left[y, \tilde{R}, r\right]^T$, $\boldsymbol{\gamma} \stackrel{\text{def}}{=} [\gamma_1, \gamma_2, \gamma_3]^T$.

Remark 3: The proof validating the DMRAC design is provided in [26].

The reference model encodes the optimized (offline) closed-loop system behavior by:

$$(a_\text{m}, b_\text{m})^* = \arg \min_{(a_\text{m}, b_\text{m}) \in \Omega_\text{rm}} J_\text{m}(a_\text{m}, b_\text{m}), \tag{20}$$

where J_m is selected analogously to the tracking error term in (14) with the model output y_m obtained using (10) with (a_m, b_m) prescribed by the optimization algorithm. The problem feasible set Ω_rm is obtained by translating the Σ_A into the reference model parameter space as:

$$\Omega_\text{rm} \stackrel{\text{def}}{=} \left\{ (a_\text{m}, b_\text{m}) : a_\text{m} < \frac{\hat{R}_\text{op} + b_\text{m} r_\text{op}}{y_\text{op}} \right. \\ \left. \wedge a_\text{m} > -\frac{u_\text{max} b_\text{p op} - \hat{R}_\text{op} - b_\text{m} r_\text{op}}{y_\text{op}} \right\}, \tag{21}$$

where r_op, y_op, $\hat{R}_\text{op}$ and $b_\text{p op}$ denote the nominal values at the operating point.

The online parameter adaptation rate gains, used in (16), are selected as:

$$\boldsymbol{\gamma}^* = \arg \min_{\boldsymbol{\gamma} \in \Omega_\gamma} J_\gamma(\boldsymbol{\gamma}), \tag{22}$$

where J_γ is selected analogously to previous task with the process output y obtained by closing the loop over Σ_SBR using $\Sigma_\text{DO-DMRAC}$. The problem feasible set Ω_γ ensures positive definiteness of $\boldsymbol{\gamma}$.

Combining (16) and (19) equipped with $\boldsymbol{\gamma} = \boldsymbol{\gamma}^*$ and $(a_\text{m}, b_\text{m}) = (a_\text{m}, b_\text{m})^*$ yields the $\Sigma_\text{DO-DMRAC}$ emulated to discrete-time using forward Euler method. Finally, the control signal is applied to the plant as in (12).

V. EXPERIMENT

In Section V-A the experiment setup is provided. Results and discussion are delivered in Section V-B.

A. Setup

Let Σ_SBR be the implemented initially calibrated simulation model of SBR at Swarzewo in Northern Poland (Section III-A). To predict the plant's behavior over the experiment horizon $T_\text{E} = 1.25\,\text{d}$, a set of complementary model parameters was used: $R_{20} = 16\,\text{g}_{\text{O}_2}/\text{m}^4$, $h_\text{diff} = 0.5\,\text{m}$, $V_\text{max} = 4948\,\text{m}^3$, $a = 0.8$, $u_\text{max} = 80\,\text{m}^3/\text{min}$, and $C_{\text{O}_2\,\text{sat}}$ cubic approximation coefficients $a_0 = 13.89$, $a_1 = 0.3825$, $a_2 = 0.007311$, $a_3 = -0.00006588$.

The disturbance input trajectories over T_E, which include the quality of wastewater in the SBR retention tank (COD, TN, TP) as well as the operating temperature ($T(t)$, $\forall t$) are illustrated in top two plots in Fig. 4. The input scenario was developed by phenomenological modeling to match the Swarzewo daily operational conditions. The bottom plot (Fig. 4) details the Swarzowo SBR duty cycle. It comprises three alternating sequences of aerobic and anaerobic phases characterized by different duration and interrupted by refills.

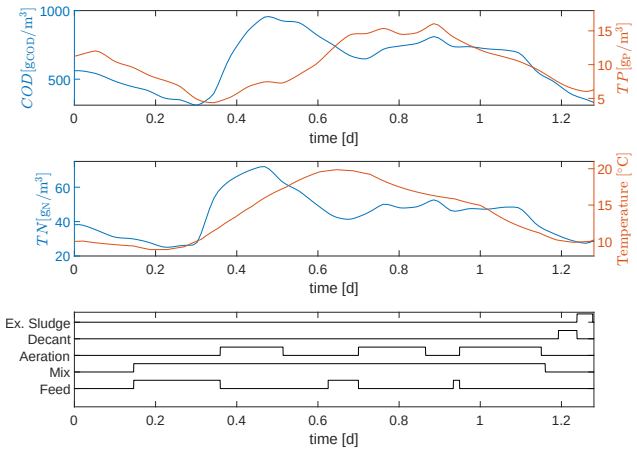

Fig. 4. Characteristics of the inflow at the horizon of the SBR cycle.

The NMPC algorithm configuration includes $\rho_\varepsilon = 100$, $T_\text{s} = 1\,\text{min}$, and $N = 30$.

The DMRAC algorithm configuration includes: $T_\text{s} = 1\,\text{s}$, $(a_\text{m}, b_\text{m})^* = (520.28, 520.28)$ and $\boldsymbol{\gamma}^* = [199.97, 0.0182, 0.1]^T$.

These parameters were calculated by offline optimization using the GlobalSearch Algorithm which is part of the Matlab Global Optimization Toolbox, with a view to ensuring that solutions were not on the constraints.

B. Results and discussion

In Fig. 5, the DO concentration control performance over single duty cycle (T_{E}) is presented. The top plot indicates the controllers ability to track the desired DO reference trajectory. The bottom plot illustrate the generated control signals ($Q_{\mathrm{air}} \equiv u(t)$) and estimated $\hat{R}$.

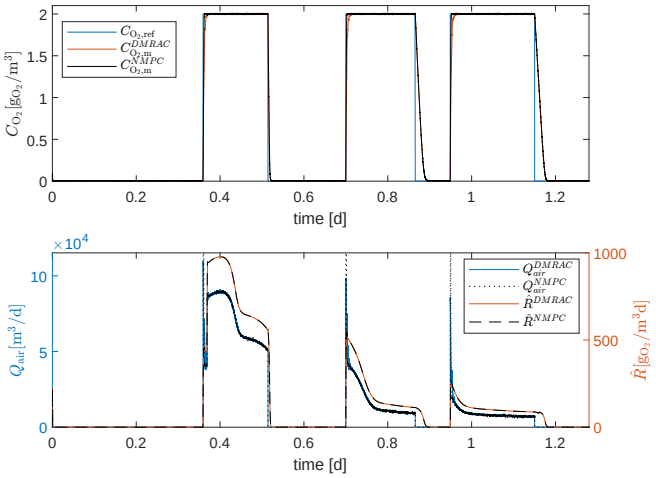

Fig. 5. Control results.

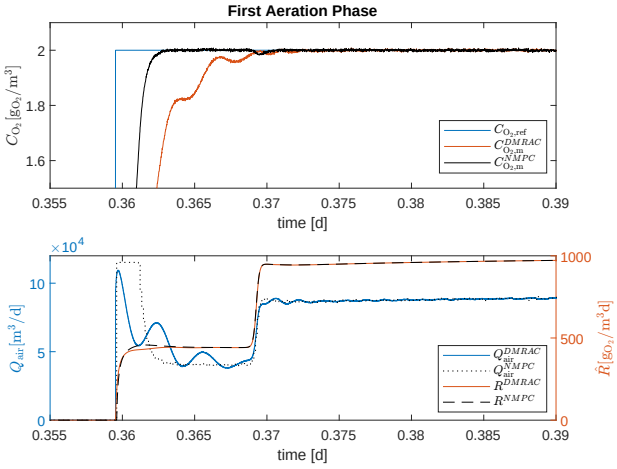

Fig. 6. Transients in the first aeration phase.

Due to small differences in the corresponding trajectories a zoom in on the transient states of the first and second aeration phases are shown in Fig. 6 and Fig. 7. Although, both controllers target to minimize the quadratic performance index, some discrepancies are observed. This is mainly due to structure differences of the internal NMPC model and DMRAC reference model. The DMRAC algorithm has a lower initial control quality than NMPC. This is due to the adaptation mechanism that has to adjust the new operating conditions, which is done recursively in each step. On the other hand, the NMPC can perform many iterations over a sampling period. During subsequent aeration phases, smaller parameter adjustments are required, allowing the algorithm to follow the reference signal more closely at the start of the second and third aeration phase. Also, it is worth mentioning that the spikes visible in the figures are on the scale of days. Thus, their duration is relatively long considering the dynamics of the actuator, which time constants are counted in seconds or minutes. Therefore, it is not considered as challenging for the aeration system.

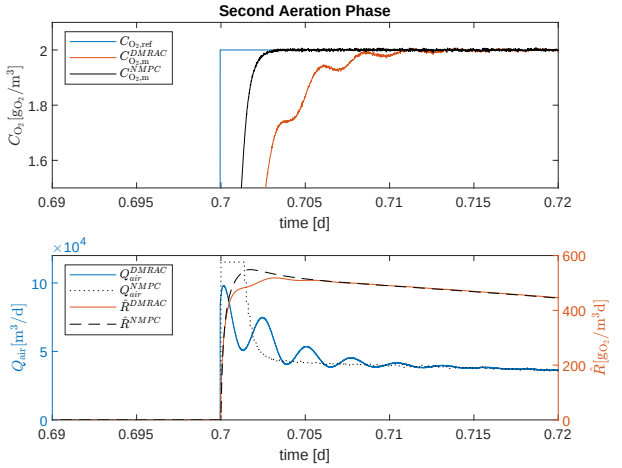

Fig. 7. Transients in the second aeration phase.

The internal behavior of algorithms is illustrated by plotting the trajectories of DMRAC's parameters and NMPC's additive error term in Fig. 8. These parameters are only determined if the algorithm is active, i.e., during the aeration phases (see Fig. 4 graph 3). It is observed that DMRAC tends to resemble more oscillatory behavior. This is due to the structure of the adaptive algorithm, where the signals and parameters change in successive moments of the algorithm's operation. Also, the parameters change significantly at the beginning of the aeration phase. Similarly to the respiration values. In turn, the NMPC internal model response deviates from the measurement at the beginning of the aerobic phase, thereafter it is close to measurement noise.

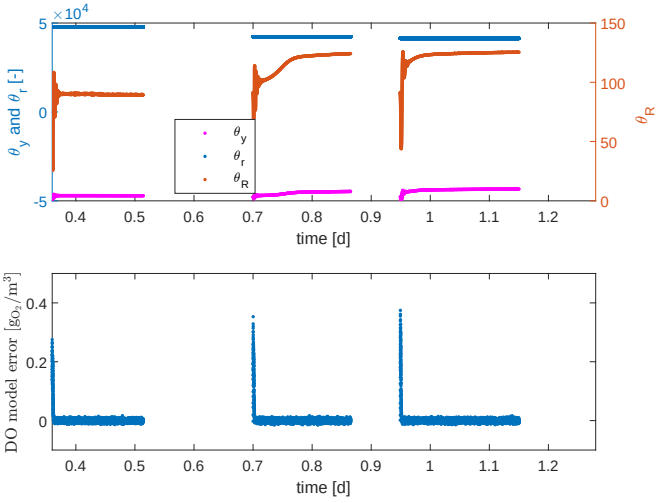

Fig. 8. DMRAC parameter adaptation and NMPC model error.

In Fig. 9, the COD, TN, and TP have been plotted with the

evolution of DO to illustrate the treatment due to aeration. It should be noted that around $1.2\,\mathrm{d}$ the decantation phase takes place and is responsible for the last decreasing slope of the trajectories.

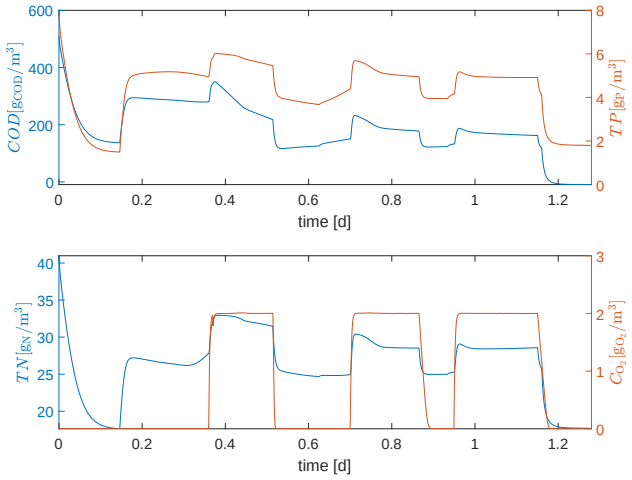

Fig. 9. The treatment performance over T_{E}.

The performance of the controllers has been assessed by providing the Integral Squared Error (ISE), L_2 and L_∞ norms, and Root Mean Square (RMS). In addition, the Control Energy, understood in terms of integral of the square of the normalized control signal $(u/u_{\max})^2$, has been evaluated. The results of the assessment have been collated in Table I.

The results illustrate that both controllers operate at comparable performance considering the ISE and RMS indicators. Therefore, in both cases the control error has a comparable impact on the system behavior. The NMPC controller appears to generate slightly higher control costs compared to DMRAC, suggesting that DMRAC may be more energy efficient. This is clearly the result of the optimization task formulation which in case of the NMPC lacks the term accounting for the energy in the control signal. The L_2 and L_∞ norms appear to be similar for both controllers, suggesting that both perform similarly in terms of maximum and average control error values.

VI. CONCLUSIONS

This paper addressed the problem of optimizing the control of the aeration process in a WRRF treatment plant based on SBR technology. Two approaches based on algorithms developed using NMPC and DMRAC were proposed. It was shown that both algorithms are suitable for achieving optimized DO control. In the case of the NMPC algorithm, the quality index is optimized directly in each step of the algorithm. In turn, the influence of uncertainty was reduced by a feedback mechanism and accounted for using an additive inner model member on a sliding prediction horizon. In DMRAC algorithm, the optimal behavior of the closed-loop control system with respect to the assumed quality index was encoded in the form of a reference model. Influence of uncertainty is reduced by updating the control law gain, aiming to ensure that the control system reflects the behavior of the reference model. This action is enhanced by optimizing the parameters of the adaptation mechanism. Experiments conducted on a pre-calibrated SBR model of Swarzewo illustrate the above observations.

TABLE I

OPTIMIZATION RESULTS TABLE FOR DIFFERENT CONTROLLERS WITH PHASE-WISE BREAKDOWN

Controller	Integral Squared Error (ISE)			
	Phase-wise			Total
	First	Second	Third	
NMPC	7.78×10^{-3}	2.71×10^{-2}	3.33×10^{-2}	6.84×10^{-2}
DMRAC	8.90×10^{-3}	2.86×10^{-2}	3.52×10^{-2}	7.29×10^{-2}
Controller	Control Energy			
	Phase-wise			Total
	First	Second	Third	
NMPC	6.08×10^{-2}	6.78×10^{-3}	2.56×10^{-3}	7.01×10^{-2}
DMRAC	6.03×10^{-2}	6.30×10^{-3}	1.99×10^{-3}	6.85×10^{-2}
Controller	L_2 norm			
	Phase-wise			Total
	First	Second	Third	
NMPC	26.01	48.42	53.70	76.98
DMRAC	27.73	49.76	55.17	79.40
Controller	L_∞ norm			
	Phase-wise			Total
	First	Second	Third	
NMPC	2.00	2.00	2.00	2.00
DMRAC	2.00	2.00	2.00	2.00
Controller	Root Mean Square (RMS)			
	Phase-wise			Total
	First	Second	Third	
NMPC	0.21	0.38	0.37	0.24
DMRAC	0.23	0.39	0.38	0.25

Despite achieving comparable performance, both algorithms have their own strengths and weaknesses. While NMPC requires more computational resources, DMRAC with its lower computational complexity introduces additional oscillations into the system. Therefore, it is up to the user to decide which solution is more suitable for their needs — considering the natural process dynamics.

Future work aims to develop formal evaluation to demonstrate the extent and conditions of validity of the above observations.

REFERENCES

[1] A. Dutta and S. Sarkar, "Sequencing batch reactor for wastewater treatment: recent advances," *Current Pollution Reports*, vol. 1, no. 3, pp. 177–190, 2015.

[2] S. M. A. Masoudi, A. Hedayati Moghaddam, J. Sargolzaei, A. Darroudi, and V. Zeynali, "Investigation and optimization of the snd–sbr system for organic matter and ammonium nitrogen removal using the central composite design," *Environmental Progress & Sustainable Energy*, vol. 37, no. 5, pp. 1638–1646, 2018.

[3] S. I. Ali, M. H. Moustafa, M. S. Nwery, N. S. Farahat, and F. Samhan, "Evaluating the performance of sequential batch reactor (SBR & ASBR) wastewater treatment plants, case study," *Environmental Nanotechnology, Monitoring & Management*, vol. 18, p. 100745, 2022.

[4] R. L. Irvine, L. H. K. Jr., and T. Asano, "Sequencing batch reactors for biological wastewater treatment," *Critical Reviews in Environmental Control*, vol. 18, no. 4, pp. 255–294, 1989.

[5] J. Keller, S. Watts, W. Battye-Smith, and R. Chong, "Full-scale demonstration of biological nutrient removal in a single tank SBR process," *Water Science and Technology*, vol. 43, no. 3, pp. 355–362, 02 2001.

[6] M. A. Brdys and B. Ulanicki, *Operational control of water systems : structures, algorithms, and applications / M.A. Brdys, B. Ulanicki*. Prentice Hall New York, 1994.

[7] V.-M. Cristea, C. Pop, and P. S. Agachi, "Model predictive control of the waste water treatment plant based on the benchmark simulation model no.1-BSM1," in *Computer Aided Chemical Engineering*, ser. 18 European Symposium on Computer Aided Process Engineering, B. Braunschweig and X. Joulia, Eds. Elsevier, 2008, vol. 25, pp. 441–446.

[8] G. Harja, G. Vlad, and I. Nascu, "MPC advanced control of dissolved oxygen in an activated sludge wastewater treatment plant," in *2016 IEEE International Conference on Automation, Quality and Testing, Robotics (AQTR)*, 2016, pp. 1–6.

[9] M. Francisco, P. Vega, and S. Revollar, "Model predictive control of BSM1 benchmark of wastewater treatment process: A tuning procedure," in *2011 50th IEEE Conference on Decision and Control and European Control Conference*, 2011, pp. 7057–7062, ISSN: 0743-1546.

[10] G. Kandare and A. Nevado Reviriego, "Adaptive predictive expert control of dissolved oxygen concentration in a wastewater treatment plant," *Water Science and Technology: A Journal of the International Association on Water Pollution Research*, vol. 64, no. 5, pp. 1130–1136, 2011.

[11] N. Boruah and B. Roy, "Event triggered nonlinear model predictive control for a wastewater treatment plant," *Journal of Water Process Engineering*, vol. 32, p. 100887, 2019.

[12] U. Jeppsson, C. Rosen, J. Alex, J. Copp, K. Gernaey, M.-N. Pons, and P. Vanrolleghem, "Towards a benchmark simulation model for plant-wide control strategy performance evaluation of WWTPs," *Water Science and Technology*, vol. 53, no. 1, pp. 287–295, 01 2006. [Online]. Available: https://doi.org/10.2166/wst.2006.031

[13] H.-G. Han, Z. Liu, and J.-F. Qiao, "Fuzzy neural network-based model predictive control for dissolved oxygen concentration of WWTPs," *International Journal of Fuzzy Systems*, vol. 21, no. 5, pp. 1497–1510, 2019.

[14] P. Stentoft, T. Munk-Nielsen, J. Møller, H. Madsen, B. Valverde-Pérez, P. Mikkelsen, and L. Vezzaro, "Prioritize effluent quality, operational costs or global warming? – using predictive control of wastewater aeration for flexible management of objectives in wrrfs," *Water Research*, vol. 196, p. 116960, 2021.

[15] M. Brdys and K. Konarczak, "Dissolved oxygen control for activated sludge processes," *IFAC Proceedings Volumes*, vol. 34, no. 8, pp. 539–544, 2001.

[16] M. Li and M. Brdys, "Direct model reference adaptive control of nutrient removal at activated sludge wastewater treatment plant," in *2015 20th International Conference on Methods and Models in Automation and Robotics (MMAR)*, 2015, pp. 608–613.

[17] K. Blaszkiewicz, R. Piotrowski, and K. Duzinkiewicz, "A model-based improved control of dissolved oxygen concentration in sequencing wastewater batch reactor," *Studies in Informatics and Control*, vol. 23, no. 4, 2014.

[18] P. Hirsch, R. Piotrowski, and K. Duzinkiewicz, "Two-step model based adaptive controller for dissolved oxygen control in sequencing wastewater batch reactor," in *2015 20th International Conference on Methods and Models in Automation and Robotics (MMAR)*, 2015, pp. 677–682.

[19] R. Piotrowski, "Supervisory fuzzy control system for biological processes in sequencing wastewater batch reactor," *Urban Water Journal*, vol. 17, no. 4, pp. 325–332, 2020.

[20] T. Zubowicz, "Decentralized tracking of dissolved oxygen concentration in interacting multi zone bioreactor by supervised PI controller," Ph.D. dissertation, Gdańsk University of Technology, Gdańsk, Poland, 2018. [Online]. Available: https://www.worldcat.org/title/1117293048

[21] S. Puig, L. Corominas, A. Traore, J. Colomer, M. Balaguer, and J. Colprim, "An on-line optimisation of a SBR cycle for carbon and nitrogen removal based on on-line pH and OUR: the role of dissolved oxygen control," *Water Science and Technology*, vol. 53, no. 4-5, pp. 171–178, 02 2006.

[22] M. Czyżniewski, R. Łangowski, and R. Piotrowski, "Respiration rate estimation using non-linear observers in application to wastewater treatment plant," *Journal of Process Control*, vol. 124, pp. 70–82, 2023.

[23] T. Ujazdowski, T. Zubowicz, and R. Piotrowski, "A comprehensive approach to SBR modelling for monitoring and control system design," *Journal of Water Process Engineering*, vol. 53, p. 103774, 2023.

[24] J. Rossiter, *Model-Based Predictive Control: A Practical Approach*. CRC Press, 2003.

[25] P. Tatjewski, "Model-based predictive control," in *Advanced Control of Industrial Processes: Structures and Algorithms*, ser. Advances in Industrial Control, 2007, pp. 107–271.

[26] J. Slotine and W. Li, *Applied Nonlinear Control*, ser. Prentice-Hall International Editions. Prentice-Hall, 1991. [Online]. Available: https://books.google.pl/books?id=HddxQgAACAAJ